

Electronic Supporting Information (ESI)

Bipyrazole bearing ten nitro groups – novel highly dense oxidizer for forward-looking rocket propulsions

Igor L. Dalinger,[‡] Kyrill Yu. Suponitsky,[‡] Tatyana K. Shkineva,[‡] David B. Lempert,[§] and Aleksei B. Sheremetev^{*‡}

[‡] *N. D. Zelinsky Institute of Organic Chemistry, Russian Academy of Sciences,
Moscow 119991, Russian Federation,*

[‡] *A. N. Nesmeyanov Institute of Organoelement Compounds, Russian Academy of Sciences,
Moscow 119991, Russian Federation,*

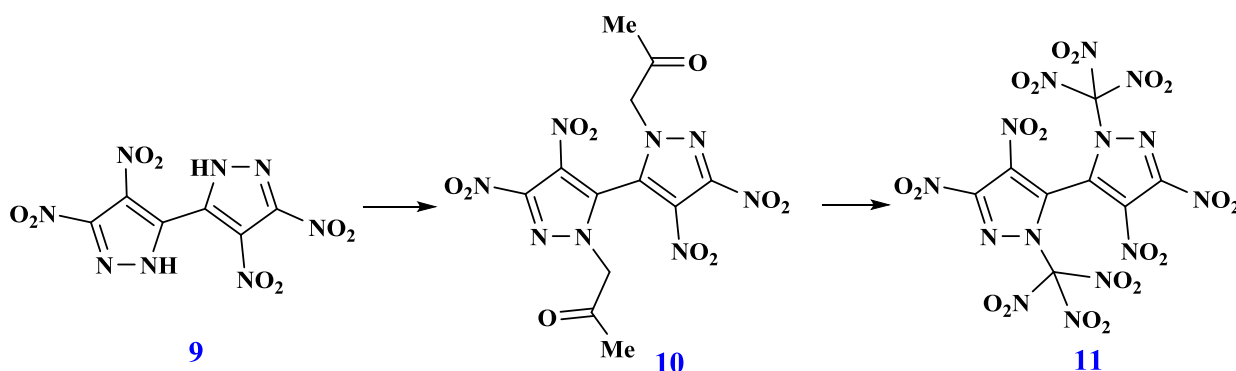
[§] *Institute of Problems of Chemical Physics, Russian Academy of Sciences,
Chernogolovka, Moscow region, 142432 Russian Federation*

Table of Contents

Experimental procedures	2
Computational Part	5
List of densest crystal structures	6
Molecular and Crystal Structure of Compound 11 based on X-ray and DFT Data	8
References	14
NMR Spectra	16

Experimental Procedures

All the reagents were of analytical grade, purchased from commercial sources, and used as received. The ^{13}C , and ^{14}N NMR spectra for compound **11** were recorded on a Bruker DRX-500 NMR spectrometer at 125.76 and 36.14 MHz respectively; over spectra were recorded on a Bruker AM-300 instrument at 300.13, 75.47, and 30.40 MHz, respectively. Chemical shifts for ^1H and ^{13}C NMR spectra are reported relative to $(\text{CH}_3)_4\text{Si}$, and ^{14}N and ^{15}N NMR to nitromethane. Infrared (IR) spectra were determined in KBr pellets on a Bruker ALPHA spectrometer. Melting point for compound **10** was determined by Kofler method on a Boetius bench (heating rate $4^\circ/\text{min}$) and was not corrected. Thermal stability of compound **11** was investigated with differential scanning calorimetry (DSC 204 HP, Netzsch). Elemental analyses (C, H, N) were obtained by using a CHNS/O Analyzer 2400 (Perkin–Elmer instruments Series II). Analytical TLC was performed using commercially pre-coated silica gel plates (Merck Silica gel 60 F₂₅₄), and visualization was effected with short-wavelength UV-light.



2,2'-Diacetyl-4,4',5,5'-tetranitro-2H,2'H-3,3'-bipyrazole (10). Bipyrazole **9** [1] (1 g, 3 mmol) was dissolved in MeOH (10 ml) and a solution of sodium bicarbonate (0.59 g, 7 mmol) in water (18 ml) was added. After stirring 30 min at room temperature, bromoacetone (0.66 ml, 8 mmol) was added dropwise and the reaction mixture was stirred for 3 days at room temperature. The precipitate was collected by filtration, washed with water (5 mL) and air-dried. Yield 1.22 g (82%) light beige solid. T_{dec} 245 $^\circ\text{C}$ (dichloroethane). ^1H NMR (DMSO- d_6 , δ): 5.61 (s, 1 H CH_2); 5.60 (s, 1 H CH_2); 2.16 (s, 3 H, CH_3) ppm. ^{13}C NMR (DMSO- d_6 , δ): 200.58 (CO), 148.62 (C3); 128.73 (C4); 128.36 (C5); 62.19 (CH_2); 28.19 (CH_3) ppm. ^{14}N NMR (DMSO- d_6 , δ): -28.75 (NO_2) ppm. IR (KBr): ν = 1740 (m); 1556 (s), 1488 (m), 1418 (w), 1360 (m), 1328 (m), 1176

(w), 1176 (w), 810 (m) cm^{-1} . Elemental analysis for $\text{C}_{12}\text{H}_{10}\text{N}_8\text{O}_{10}$ (426.26). Calcd: C 33.81; H 2.36; N 26.29 %. Found: C 33.44; H 2.52; N 25.94 %.

4,4',5,5'-Tetranitro-2,2'-bis(trinitromethyl)-2H,2'H-3,3'-bipyrazole (11). A solution of compound **10** (0.7 g, 1.6 mmol) in 100% H_2SO_4 (6 ml) was stirred at 5–10 °C and treated by dropwise addition of HNO_3 ($d = 1.5 \text{ g/cm}^3$, 5 ml) and the mixture was stirred for 4 days at room temperature. Separated crude product was filtered off, washed with $\text{CF}_3\text{CO}_2\text{H}$ (3 ml), dried over P_2O_5 . The solution was poured ice water (40 ml), extracted with ether (3 x 20 ml). The organic phase was washed with water, dried over MgSO_4 , and the solvent removed in *vacuo*. Both solids were combined and pure compound **11** (0.6 g, 61%) was isolated as light-yellow crystals by recrystallization from CHCl_3 . M.p. 123 °C, $T_{\text{d(onset)}}$ 125 °C. ^{13}C NMR (acetone- d_6 , δ): 151.07 (C3, br.s); 134.83 (C4, br.s); 130.51 (C5); 120.45 (C(NO $_2$) $_3$, br.s) ppm. ^{14}N NMR (acetone- d_6 , δ): –37.33 (C $_{\text{Pz}}$ –NO $_2$); –42.29 (C–(NO $_2$) $_3$) ppm. IR (KBr): $\nu = 1641$ (s), 1621 (os), 1610 (s), 1584 (s), 1566 (s), 1528 (m), 1347 (m), 1321 (m), 1274 (s), 1212 (w), 860 (w), 832 (w), 805 (s), 793 (s) cm^{-1} . Elemental analysis for $\text{C}_8\text{N}_{14}\text{O}_{20}$ (612.17). Calcd: C 15.70; N 32.03 %. Found: C 15.66; N 31.90 %.

Single crystal X-ray study. X-ray experiments for compound **11** was carried out using SMART APEX2 CCD ($\lambda(\text{Mo-K}\alpha)=0.71073 \text{ \AA}$, graphite monochromator, ω -scans) at 100K and room temperature (298K). Collected data were processed by the SAINT и SADABS programs incorporated into the APEX2 program package [2]. The room and low temperatures structures were solved by the direct methods and refined by the full-matrix least-squares procedure against F^2 in anisotropic approximation. The refinement was carried out with the SHELXTL program [3]. The details of data collection and crystal structures refinement are summarized in Table 1S along with CCDC numbers which contain the supplementary crystallographic data for this paper. These data can be obtained free of charge via www.ccdc.cam.ac.uk/data_request/cif.

Table 1S. Crystallographic data for compound **11** at 100K and room temperature.

	11 (100K)	11 (298K)
formula	C ₈ N ₁₄ O ₂₀	C ₈ N ₁₄ O ₂₀
fw	612.22	612.22
crystal system	Monoclinic	Monoclinic
space group	<i>P2₁/n</i>	<i>P2₁/n</i>
<i>a</i> , Å	9.7746(9)	9.9011(13)
<i>b</i> , Å	10.4557(10)	10.5386(13)
<i>c</i> , Å	19.0490(17)	19.291(2)
β , deg.	91.034(2)	91.071(3)
<i>V</i> , Å ³	1946.5(3)	2012.6(4)
<i>Z</i>	4	4
<i>d</i> _{cryst} , g·cm ⁻³	2.089	2.021
<i>F</i> (000)	1224	1224
μ , mm ⁻¹	0.209	0.202
θ range, deg.	2.14 – 30.00	2.11 – 29.02
reflections collected	33948	24502
independent reflections / <i>R</i> _{int}	5680 / 0.0429	5351 / 0.0431
Completeness to theta θ , %	100%	99.8%
refined parameters	379	379
<i>GOF</i> (<i>F</i> ²)	1.047	1.046
reflections with <i>I</i> > 2 σ (<i>I</i>)	4553	3450
<i>R</i> ₁ (<i>F</i>) (<i>I</i> > 2 σ (<i>I</i>)) ^a	0.0369	0.0462
<i>wR</i> ₂ (<i>F</i> ²) (all data) ^b	0.0970	0.1302
Largest diff. peak/hole, <i>e</i> ·Å ⁻³	0.468 / -0.287	0.304 / -0.236
CCDC number	1837840	1837841

^a $R_1 = \sum |F_o - |F_c|| / \sum (F_o)$; ^b $wR_2 = (\sum [w(F_o^2 - F_c^2)^2] / \sum [w(F_o^2)^2])^{1/2}$

Computational Part

Geometry optimization of isolated molecule was carried out at M052X/6-311G(df,pd) level of theory that was successfully utilized in our recent studies on polynitro compounds [4-6]. The GAUSSIAN program was used for calculation [7]. The wave function obtained from calculation of isolated molecule was analyzed in terms of R. Bader "AIM" topological theory [8] using the AIMALL program [9]. Estimation of energies of intramolecular nonbonded interactions (E_{cont}) was based on correlation of E_{cont} with the potential energy density ($V(r)$) in BCP ($E_{\text{cont}} = \frac{1}{2}V(r)$). [10-11].

Crystal packing analysis was carried out using two methods. The first one is based on combination of geometrical and energetic approaches, and was adopted in our recent studies on high energetic compounds [4-6,12]. It is based on analysis of close and shortened intermolecular contacts between central molecule and its closest environment in the crystal, and estimation of interaction energy between central molecule and each molecule from its closest environment (pair interaction energies). Molecule is included in the closest environment if at least one atom...atom contact is shorter than sum of van-der-Waals radii [13] plus 0.5 Å. All found intermolecular contacts are separated into three subgroups according to interatomic distances (d_{1-2}): 1) ordinary van-der-Waals contacts ($d_{1-2} > r_{\text{vdw1}} + r_{\text{vdw2}} + 0.05 \text{ Å}$), 2) shortened contacts ($r_{\text{vdw1}} + r_{\text{vdw2}} + 0.05 \text{ Å} > d_{1-2} > r_{\text{vdw1}} + r_{\text{vdw2}} - 0.1 \text{ Å}$), 3) close contacts ($d_{1-2} < r_{\text{vdw1}} + r_{\text{vdw2}} - 0.1 \text{ Å}$). Here, r_{vdw1} and r_{vdw2} are van-der-Waals radii of corresponding atoms. Only shortened and close contacts are given in Table 3S.

Interaction energy of a molecular pair (dimer) was estimated according to well-known general formula $E_{\text{int}} = E_{\text{AB}} - E_{\text{A}} - E_{\text{B}}$, where E_{AB} – energy of a dimer, and E_{A} , E_{B} – energies of isolated molecules from which this dimer consists of. In the case of compound **11** which contains one symmetrically independent molecule in the unit cell, $E_{\text{A}} = E_{\text{B}}$. For E_{int} estimation, the structures of a dimer and isolated molecule were taken from the low temperature X-ray data without further optimization. The BSSE correction was taken into account.

The second approach for crystal packing analysis was based on recently proposed Δ_{OED} (overlap of electron density) criterion [6]. It is assumed that upon crystal formation, molecules interact to each other by means of overlap of their electron densities. It means that volume of isolated molecule is larger than that of the molecule in a crystal. Similarly, density of isolated molecule (d_{mol}) is lower than that in a crystal (d_{cryst}). The latter is the density of the crystal packing obtained from X-ray experiment. The value of d_{mol} can be estimated by analysis of the electron density of optimized isolated molecule in term of the AIM theory. It is defined as a ratio of molecular mass per molecular volume (the latter is presented as the sum of atomic volumes)

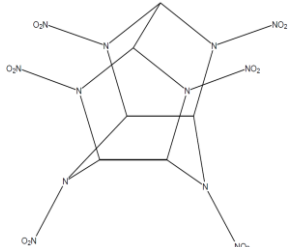
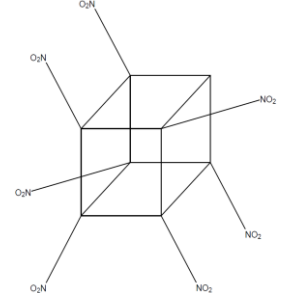
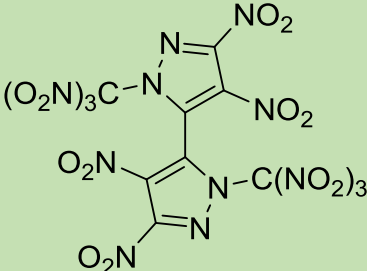
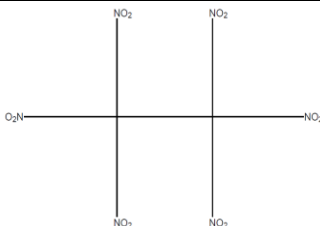
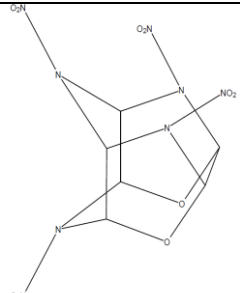
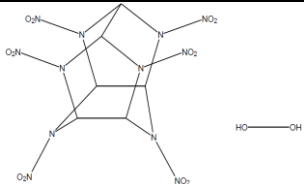
$$d_{\text{mol}} = m_{\text{mol}}/V_{\text{mol}} ; \quad m_{\text{mol}} = M_{\text{mol}}/N_{\text{A}} ; \quad V_{\text{mol}} = \sum_i V_{\text{at}}^{(i)}.$$

Here, M_{mol} and m_{mol} are molar and molecular masses, respectively, N_{A} is Avogadro number, V_{mol} and V_{at} are molecular and atomic volumes, respectively. It is convenient to present d_{mol} in g/cm^3 units. Evidently, the volume and density of any molecular fragment can be calculated in a similar way. For estimation of V_{mol} , isodensity surface of $0.0004 \text{ e}/a_0^3$ (a_0 – Bohr radius) was utilized for integration procedure. So estimated molecular volume comprises about 99.8% of all electrons (nearly whole molecule), and charge leakage does not exceed $0.002 \text{ e}/\text{\AA}^3$ that approximately corresponds to numerical error of integration of calculated electron density. It is evident, that difference between crystal and molecular density can be served as a measure of how pronounced is the overlap of molecular electron densities upon crystal structure formation. Therefore, the Δ_{OED} criterion defined as $\Delta_{\text{OED}} = d_{\text{cryst}} - d_{\text{mol}}$ would characterize tightness of crystal packing. Combined analysis of d_{mol} and Δ_{OED} values would clarify an origin of the observed crystal packing density.

List of densest crystal structures

In Table 2S, we provided list of the densest crystal structures taken from the search of Cambridge Structural Database [14] for compound containing C, N, O, H atoms, which density at room temperature (298K) and normal pressure is higher than $2.000 \text{ g}/\text{cm}^3$. For those experiments which were carried out at low temperature, density was recalculated based on the results of X-ray studies of polynitro compounds and high nitrogen heterocycles at 100K and room temperature. It appears that decrease of density from 100 to 298K vary in narrow range (3-4%). Densities were recalculated using 3.5% as average value in assumption of linear dependence of density vs. temperature ($d_{\text{T}} = -kT+b$) [15].

Table 2S. List of densest crystal structures containing C, N, O, H atoms. Search in Cambridge Structural Database.

Structural formula	Exp. temp.	Space group, unit cell param.	Density ^a	Density at room temp.	Ref.
	298	$P2_1/n$ $a=8.863$ $b=12.593$ $c=13.395$ $\beta=106.92$	2.035	2.035	16
	295	$Pbcn$ $a=23.594$ $b=8.174$ $c=14.264$	2.024	2.024	17
	295	$P2_1/n$ $a=9.9011$ $b=10.5386$ $c=19.291$ $\beta=91.071$	2.021	2.021	This work
	145	$P2_1/c$ $a=10.152$ $b=9.311$ $c=10.251$ $\beta=97.54$	2.075	2.020	18
	295	$P3_1$ $a=11.086$ $b=11.086$ $c=8.137$ $\gamma=120.0$	2.014	2.014	19
	85	$Pbca$ $a=9.475$ $b=13.154$ $c=23.427$	2.071	2.000	20

^a density is given for experimental temperature

Molecular and Crystal Structure of Compound **11** based on X-ray and DFT Data

General view of molecular structure of **11** is depicted in Figure 1S.

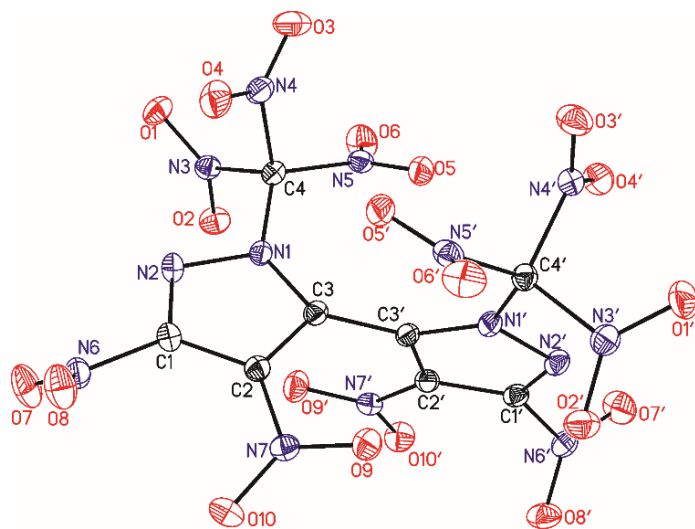


Figure 1S. General view of molecule **11** with the atom numbering scheme. Thermal ellipsoids are set at the 50% probability level.

The bipyrazole backbone adopts twisted *trans*-configuration (Table 3S). Three out of four nitrogroups (those attached directly to the pyrazole rings) are out of the plane of corresponding rings while the N7'O9'O10' group is nearly coplanar to the pyrazole. Geometry of the C(NO₂)₃ moieties somewhat deviates from ideal propeller-like structure that is frequently observed for this group [5,12]. Molecule **11** is "overloaded" with substituents and has strained structure. Many shortened intramolecular contacts are observed (Table 4S), and C3-C3' bond is elongated (Table 3S). Molecular structure of **11** can be compared to related compound **12** [21] which differ by an absence of one trinitromethyl substituent at one of the pyrazole rings (Figure 2S). Molecule **12** also has strained structure with the same C3-C3' inter-ring bond length (Tables 3S) and nonplanar geometry. The main difference between two molecules is in mutual orientation of the pyrazole rings (**12** has *cisoid* configuration) and geometry of the trinitromethyl group. Difference in orientation of the pyrazole rings is probably governed by intramolecular forces, while differences in geometry of trinitromethyl groups might be related to different crystal packing (see comparison of their crystal structures in the main text).

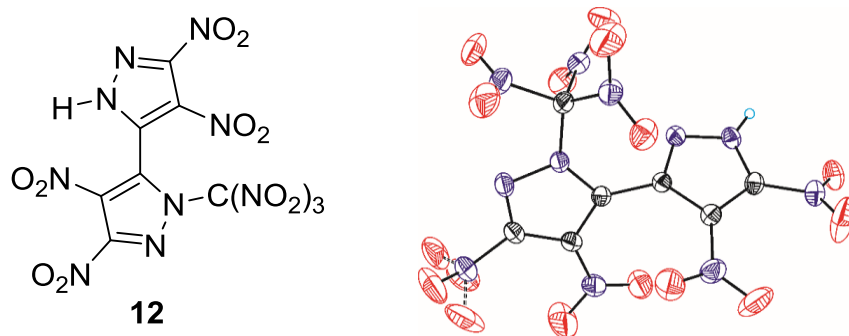


Figure 2S. General view of molecule **12**. Thermal ellipsoids are set at the 30% probability level.

Table 3S. Main geometric parameters of molecules **11** and **12**. Calculation vs. Experiment

Bond, Å or Torsion angle, deg.	11		12
	X-ray	Calculation	X-ray data
C3-C3'	1.465(2)	1.463	1.465(3)
N3-C4	1.527(2)	1.544	1.558(3)
N4-C4	1.551(2)	1.547	1.558(3)
N5-C4	1.508(2)	1.522	1.545(3)
N6-C1	1.451(2)	1.463	1.466(3)
N7-C2	1.433(2)	1.441	1.435(3)
C4-N1	1.412(2)	1.409	1.416(3)
N3'-C4'	1.539(2)	1.547	–
N4'-C4'	1.550(2)	1.555	–
N5'-C4'	1.510(2)	1.514	–
N6'-C1'	1.461(2)	1.462	1.448(3)
N7'-C2'	1.439(2)	1.454	1.436(3)
C4'-N1'	1.414(2)	1.415	–
N1-C3-C3'-N1'	117.1(2)	111.1	-56.1(4)
O7-N6-C1-N2	51.4(2)	35.4	disorder
O8-N6-C1-N2	-128.3(2)	-143.2	disorder
O9-N7-C2-C1	-155.7(2)	-153.4	173.0(3)
O10-N7-C2-C1	22.8(2)	28.0	-7.6(5)
N2-N1-C4-N3	-44.85(14)	-54.3	12.4(3)
N2-N1-C4-N4	72.63(13)	67.4	-105.2(2)
N2-N1-C4-N5	-167.35(11)	-175.5	130.2(2)
O1-N3-C4-N1	116.98(13)	127.2	-105.1(2)
O2-N3-C4-N1	-62.67(14)	-52.0	74.8(2)
O3-N4-C4-N1	161.56(11)	169.7	-152.4(2)
O4-N4-C4-N1	-19.7(2)	-9.3	28.8(3)
O5-N5-C4-N1	-53.3(2)	-66.5	10.4(3)
O6-N5-C4-N1	129.81(13)	113.6	-168.9(3)
O7'-N6'-C1'-N2'	-60.6(2)	-34.1	-31.7(3)
O8'-N6'-C1'-N2'	118.6(2)	144.6	149.3(3)
O9'-N7'-C2'-C1'	179.71(13)	143.8	159.9(3)
O10'-N7'-C2'-C1'	-0.9(2)	-37.8	-18.3(4)
N2'-N1'-C4'-N3'	-42.02(14)	-44.6	–
N2'-N1'-C4'-N4'	76.47(13)	73.9	–
N2'-N1'-C4'-N5'	-162.43(10)	-165.5	–
O1'-N3'-C4'-N1'	129.56(13)	135.5	–
O2'-N3'-C4'-N1'	-51.23(14)	-46.4	–
O3'-N4'-C4'-N1'	155.80(11)	150.3	–
O4'-N4'-C4'-N1'	-25.4(2)	-32.1	–
O5'-N5'-C4'-N1'	-54.8(2)	-59.9	–
O6'-N5'-C4'-N1'	127.42(13)	127.3	

Table 4S. List of intramolecular close and shortened nonbonded contacts (Å) for molecule **11** in X-ray and calculated geometry, and energies (kcal/mol) for contacts with BCP for calculated structure.

Entry	Atomic pair		Close or shortened contact		Energy
			X-ray	Calculation	
1	O1	O3	2.916	2.762	
2	O2	O6	2.753	2.766	
3	O2	N2	3.024	3.022	
4	O2	O9'	3.111	3.055	-1.6
5	O3	O5	3.008	2.882	
6	O4	N2	2.753	2.773	
7	O5	C3	2.941	3.030	
8	O5	O4'	2.858	2.854	-2.2
9	O5	N1'	2.899	2.893	
10	O5	N4'	3.091	2.983	
11	O5	C3'	2.633	2.722	-3.8
12	O8	O10	2.889	2.863	-2.6
13	O8	N7	—	3.113	
14	O9	O2'	2.965	3.022	-1.5
15	O9	O6'	3.017	3.042	
16	O9	N1'	3.010	3.013	
17	O9	N5'	2.875	2.904	-2.1
18	O9	C3'	2.897	2.842	
19	O10	N6	3.023	—	
20	N1	O5'	—	3.063	
21	N1	O9'	2.841	—	
22	N5	C2'	—	3.195	
23	N5	C3'	3.176	2.895	
24	C2	O5'	3.086	2.995	
25	C2	O9'	3.260	3.190	
26	C3	O5'	2.572	2.561	-5.0
27	C3	O9'	2.762	2.833	-3.1
28	C3	N5'	3.152	3.119	
29	O1'	O3'	2.898	2.918	
30	O2'	O6'	2.833	2.900	
31	O2'	N2'	2.865	2.836	
32	O3'	O5'	2.957	2.844	
33	O4'	N2'	2.830	2.775	
34	O5'	C3'	2.956	2.945	
35	O8'	O10'	2.802	2.858	-2.6
36	O8'	N7'		3.040	
37	O10'	N6'	2.873	—	

To get a deeper insight into molecular structure peculiarities of compound **11** we calculated its molecular geometry, compared it to experimental one, and studied all intramolecular nonbonded contacts. For experimental results we used experiment at low temperature as more accurate.

Calculated geometry for optimized isolated molecule somewhat deviates from experimentally observed one (the most significant deviations are found for the nitrogroups directly attached to the pyrazole rings) that is an indication of the influence of intermolecular interactions in the crystal on molecular structure. According to topological analysis of calculated electron density, for nine intramolecular contacts, bond critical points (BCPs) were localized that is an indication of attractive interaction. Data on close and shortened contacts for optimized geometry of **11** along with energies (for nine contacts) are also given in Table 4S. It can be seen, that in spite of some differences in molecular conformation (calculated vs. experimental), the system of close contacts is still nearly unchanged. It is also seen that molecule **11** has strained structure (due to a lot of repulsive close contacts), however it has also some freedom of conformational lability – an important prerequisite to tight crystal packing. Moreover, change of conformation from isolated molecule to molecule in the crystal occurs almost without breaking of the system of shortened intramolecular contacts. In the other words, rotation of substituents occurs self-consistently.

The results on close and shortened intermolecular contacts between central molecule and its closest environment for the crystal structure of compound **11** are provided in Table 5S along with pair interaction energies for corresponding dimers. Due to ten NO₂ substituents, outer surface of **11** is mostly covered by the oxygen atoms. Indeed, the results from Table 5S demonstrate that except for two molecular pairs (which connected via van-der-Waals interactions, Entries 3,4) all other 12 neighbours of the central molecule are linked to it by means of NO₂...NO₂ interactions (with small contribution from the O... π type, Entries 5,6,9,10). In spite of constrained molecular structure, there are four strong (entries 5,6,9,10) and six moderate (entries 7,8, 11-14) interactions. High packing density can be explained by the absence of the competitive types of intermolecular interactions (such as, for instance, moderate-to-strong hydrogen bonds or stacking interactions) which can impose a constraint and decrease, to some extent, freedom of movement of molecules upon crystal structure formation. In the crystal of **11**, almost all interactions are of the same type, therefore it is quite probable to expect that breaking of one O...O interaction can be compensated by formation of another one thereby resulting in very tight molecular arrangement.

Table 5S. Pair intermolecular interaction energies (kcal/mol) and close and shortened contacts (Å) of molecule of compound **11** with its closest environment in the crystal obtained at M052X/6-311G(df,pd) level of approximation.*

Entry	Close or shortened contact		Symmetry code	Distance	Energy
1	O10' O10'	O3' O6'	-1+x,y,z	2.947 2.877	-1.1
2	O3' O6'	O10' O10'	1+x,y,z	2.947 2.877	-1.1
3	No close cont		x,-1+y,z		-0.4
4	No close cont		x,1+y,z		-0.4
5	O1 O1 O2 O2 O2 O6 O10'	O9' N7' O10 C1 C2 O7 O7	1/2-x,-1/2+y,1.5-z	2.840 3.004 2.799 3.235 3.153 3.026 2.980	-6.2
6	O7 O7 O10 C1 C2 O9' N7'	O6 O10' O2 O2 O2 O1 O1	1/2-x,1/2+y,1.5-z	3.026 2.980 2.799 3.235 3.153 2.840 3.004	-6.2
7	O1 O3 O4 O4 O4 O5'	O6' O5' O8 O10 N7 O8	1.5-x,-1/2+y,1.5-z	2.812 2.963 2.945 3.022 3.033 2.730	-3.9
8	O8 O8 O10 N7 O5' O6'	O4 O5' O4 O4 O3 O1	1.5-x,1/2+y,1.5-z	2.945 2.730 3.022 3.033 2.963 2.812	-3.9
9	O5 O5 O4' O4' O4' O7' C1' C2'	O4' O7' O5 C1' C2' O5 O4' O4'	1-x,-y,2-z	2.889 2.902 2.889 3.043 3.267 2.902 3.043 3.267	-9.8

10	O9	O2'	1-x,1-y,2-z	2.856	-10.1
	O9	N2'		3.020	
	O9	C1'		3.229	
	O2'	O9		2.856	
	O6'	O8'		2.923	
	O8'	O6'		2.923	
	N2'	O9		3.020	
	C1'	O9		3.229	
11	O1	O1'	-1/2+x,1/2-y,-1/2+z	3.087	-2.3
	O7	O1'		3.053	
	O7	O3'		3.050	
	N2	O1'		3.045	
12	O1'	O1	1/2+x,1/2-y,1/2+z	3.087	-2.3
	O1'	O7		3.053	
	O1'	N2		3.045	
	O3'	O7		3.050	
13	O8	O7'	1/2+x,1/2-y,-1/2+z	3.062	-2.6
14	O7'	O8	-1/2+x,1/2-y,1/2+z	3.062	-2.6

* close contacts are given in bold, the other contacts are shortened ones

References

1. Dalinger, I. L. et al. Synthesis and physical-chemical properties of polycyclic nitropyrazoles. *Proceedings of the 29th International Annual Conference of ICT*, Karlsruhe, Germany, 57.1–57.13 (1998).
2. *APEX2* and *SAINT*. Bruker AXS Inc., Madison, Wisconsin, USA, **2009**.
3. G. M. Sheldrick, *Acta Crystallogr.* **2008**, A64, 112-122.
4. A. B. Sheremetev, B. V. Lyalin, A. M. Kozeev, N. V. Palysaeva, M. I. Struchkova, K. Y. Suponitsky, *RSC Adv.* **2015**, 5, 37617-37625.
5. I.L. Dalinger, I.A. Vatsadze, T.K. Shkineva, A.V. Kormanov, M.I. Struchkova, K.Yu. Suponitsky, A.A. Bragin, K.A. Monogarov, V.P. Sinditskii, A.B. Sheremetev, *Chem. Asian J.*, **2015**, 10, 1987-1996.
6. I.L. Dalinger, A.V. Kormanov, K.Yu. Suponitsky, N.V. Muravyev, A.B. Sheremetev, *Chem. Asian J.*, **2018**, 13, 1165-1172.
7. Frisch, M. J.; Trucks, G. W.; Schlegel, H. B.; Scuseria, G. E.; Robb, M. A.; Cheeseman, J. R.; Montgomery, J. A.; Kudin, K. N., Jr.; Burant, J. C.; Millam, J. M.; Iyengar, S. S.; Tomasi, J.; Barone, V.; Mennucci, B.; Cossi, M.; Scalmani, G.; Rega, N.; Petersson, G. A.; Nakatsuji, H.; Hada, M.; Ehara, M.; Toyota, K.; Fukuda, R.; Hasegawa, J.; Ishida, M.; Nakajima, T.; Honda, Y.; Kitao, O.; Nakai, H.; Klene, M.; Li, X.; Knox, J. E.; Hratchian, H. P.; Cross, J. B.; Bakken, V.; Adamo, C.; Jaramillo, J.; Gomperts, R.; Stratmann, R. E.; Yazyev, O.; Austin, A. J.; Cammi,

- R.; Pomelli, C.; Ochterski, J. W.; Ayala, P. Y.; Morokuma, K.; Voth, G. A.; Salvador, P.; Dannenberg, J. J.; Zakrzewski, V. G.; Dapprich, S.; Daniels, A. D.; Strain, M. C.; Farkas, O.; Malick, D. K.; Rabuck, A. D.; Raghavachari, K.; Foresman, J. B.; Ortiz, J. V.; Cui, Q.; Baboul, A. G.; Clifford, S.; Cioslowski, J.; Stefanov, B. B.; Liu, G.; Liashenko, A.; Piskorz, P.; Komaromi, I.; Martin, R. L.; Fox, D. J.; Keith, T.; Al-Laham, M. A.; Peng, C. Y.; Nanayakkara, A.; Challacombe, M.; Gill, P. M. W.; Johnson, B.; Chen, W.; Wong, M. W.; Gonzalez, C.; Pople, J. A. Gaussian 03, Revision E.01, Gaussian, Inc.: Wallingford, 2004.
8. Bader, R.F.W. *Atoms in Molecules. A Quantum Theory*, Clarendon Press, Oxford, 1990.
 9. Keith, T. A. **2014**, AIMAll, Version 14.11.23. TK Gristmill Software, Overland Park KS, USA (<http://aim.tkgristmill.com>)
 10. Espinosa, E.; Molins, E.; Lecomte, C., *Chem. Phys. Lett.* **1998**, 285, 170-173.
 11. Espinosa, E.; Alkorta, I.; Rozas, I.; Elguero, J.; Molins, E., *Chem. Phys. Lett.* **2001**, 336, 457-461.
 12. A.B. Sheremetev, N.S. Aleksandrova, N.V. Palysaeva, M.I. Struchkova, V.A. Tartakovsky, K.Yu. Suponitsky, *Chem. Eur. J.*, **2013**, 19, 12446-12457.
 13. Rowland, R.S.; Taylor, R., *J. Phys. Chem.* **1996**, 100, 7384-7391.
 14. F. H. Allen, *Acta Crystallogr., Sect. B: Struct. Sci.* **2002**, 58, 380–388. (version 5.39)
 15. A.A. Gidasov, V.A. Zalomlenkov, V.V. Bakharev, V.E. Parfenov, E.V. Yurtaev, M.I. Struchkova, N.V. Palysaeva, K.Yu. Suponitsky, D.B. Lempertd, A.B. Sheremetev, *RSC Adv.*, **2016**, 6, 34921-34934.
 16. N. B. Bolotina, M. J. Hardie, R. L. Speer Junior, A. A. Pinkerton, *J. Appl. Crystallogr.*, **2004**, 37, 808.
 - 17 M.-X. Zhang, P. E. Eaton, R. Gilardi, *Angew. Chem., Int. Ed.*, **2000**, 39, 401
 18. D. Bougeard, R. Boese, M. Polk, B. Woost, B. Schrader, (1986) *J. Phys. Chem. Solids*, **1986**, 47, 1129.
 19. Yu. V. Gatilov, T. V. Rybalova, O. A. Efimov, A. A. Lobanova, G. V. Sakovich, S. V. Sysolyatin, *J. Struct. Chem.*, **2005**, 46, 566.
 20. J. C. Bennion, N. Chowdhury, J. W. Kampf, A. J. Matzger, *Angew. Chem., Int. Ed.*, **2016**, 55, 13118.
 21. Tang, Y., He, C., Imler, G. H., Parrish, D. A. & Shreeve, J. M. *J. Mater. Chem. A*, **2018**, 6, 5136-5142.

NMR Spectra

